Electronic Supplementary Material (ESI) for RSC Advances.
This journal is © The Royal Society of Chemistry 2014

Electronic Supplementary Information

Synthesis of two copper clusters and their catalysis towards the oxidation of benzene into phenol

IR and UV–vis spectra for clusters **1** and **2**

In IR spectra of clusters **1** and **2**, the peaks at about 1607, 1489 and 1442 cm^{-1} are belonged to pyridinyl and phenol rings vibrations. The peak at 625 cm^{-1} is ascribed to Cl=O vibration of ClO_4^- groups. In MeCN solvent, the absorption bands in $\mathbf{H_2L^I}$ and $\mathbf{H_2L^{II}}$ at about 218 nm are the π–π* transition of pyridine and phenol groups; the other peaks at about 255 nm are ascribed to the n–π* transitions of ligands, Figure S1. While for clusters **1** and **2** in MeCN, the similar absorption bands at about 225 and 255 nm are also ascribed to the π–π* and n–π* transition of ligands. There are new absorption bands appearing at about 299 nm in clusters **1** and **2**, which are belonged to ligand to metal charge transfer (LMCT) absorption band. The d–d transition of Cu^{2+} ions in both clusters at the long wave range is very weak.

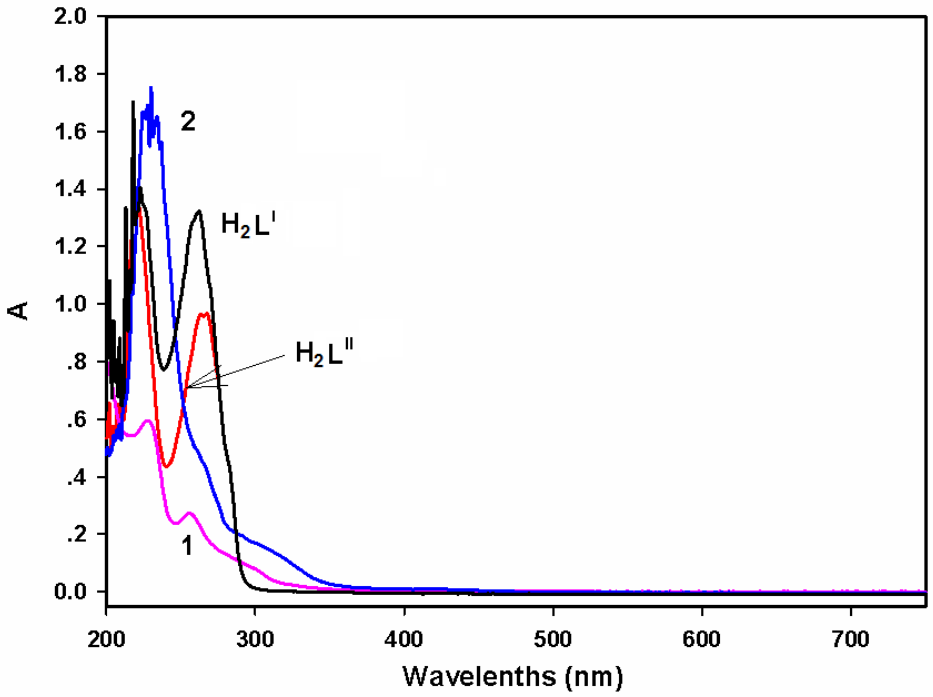

Figure S1 UV–vis absorption of ligands $\mathbf{H_2L^I}$ and $\mathbf{H_2L^{II}}$ and clusters **1**–**2** (1.0×10^{-4} mol L^{-1} in MeCN).

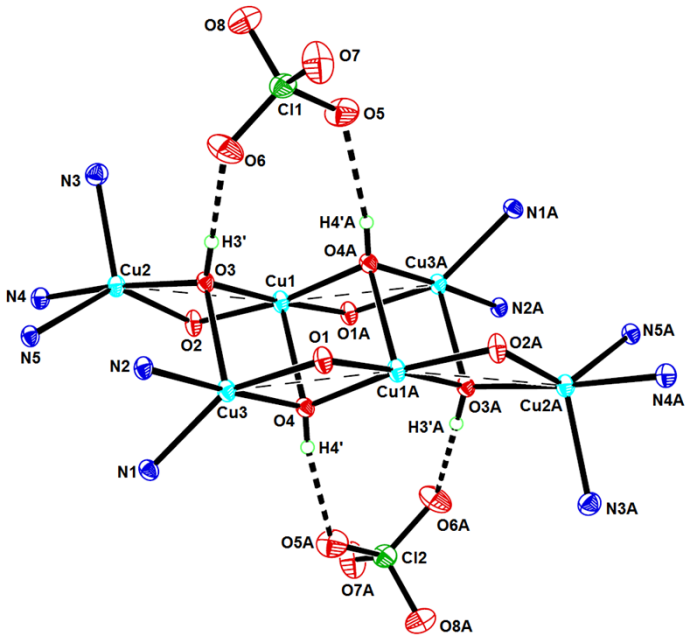

Figure S2 Six copper atoms connected with O atoms to form the two parallel three-site strings configuration, carbon atoms were omitted for clarity. Four hydrogen bonds

O–H···O connected a cation $[Cu_6(\mathbf{L^I})_2(OH)_4]^{2+}$ with two ClO_4^- anions.

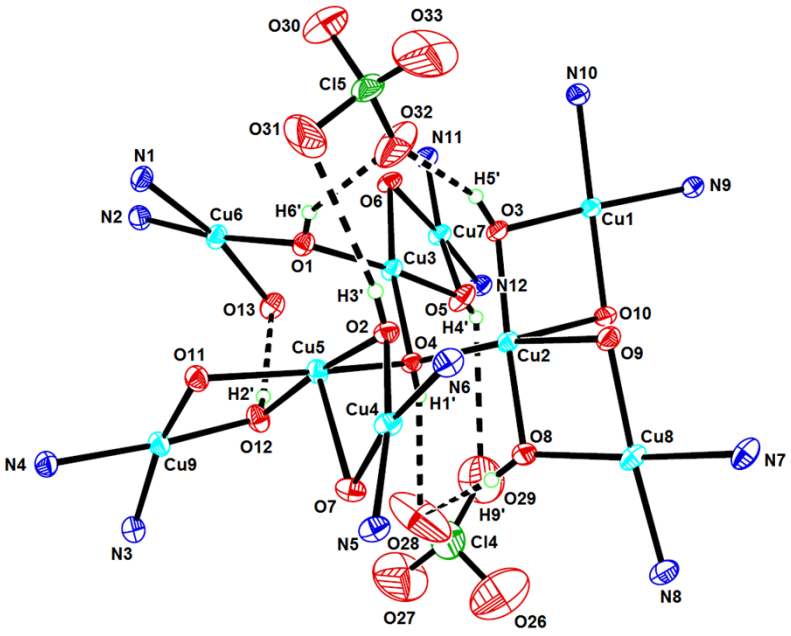

Figure S3 Six intermolecular hydrogen bonds O–H···O connected with a cation $[Cu_9(\mathbf{L^{II}})_3(OH)_7]^{5+}$ and two ClO_4^- anions, and one intramolecular hydrogen bond O5–H2'···O13 within the nonanuclear core. Carbon atoms were omitted for clarity.

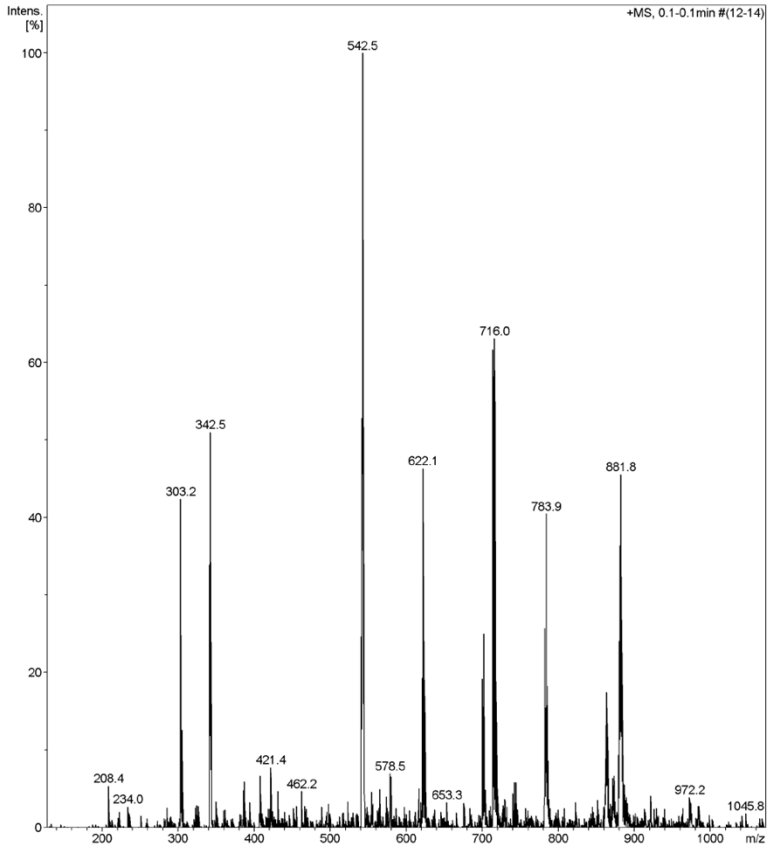
Intens.
[%]
+MS, 0.1-0.1min #(12-14)
542.5
716.0
342.5
622.1
881.8
303.2
783.9
208.4
234.0
421.4
462.2
578.5
653.3
972.2
1045.8
m/z

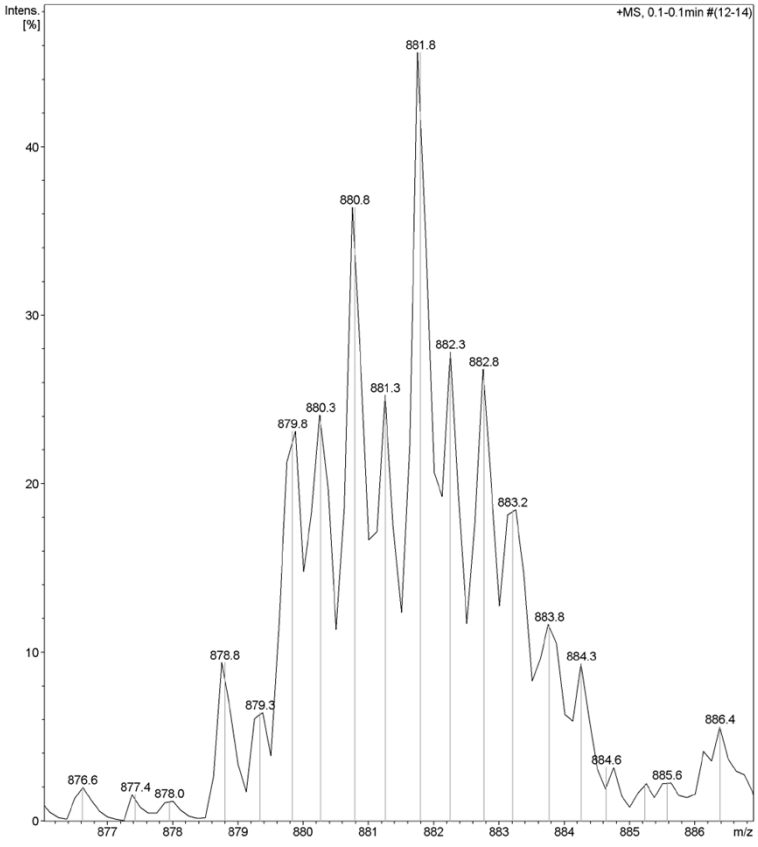
Intens.
[%]
+MS, 0.1-0.1min #(12-14)
881.8
880.8
882.3
882.8
881.3
880.3
879.8
883.2
883.8
878.8
884.3
879.3
886.4
876.6
877.4
878.0
884.6
885.6
m/z

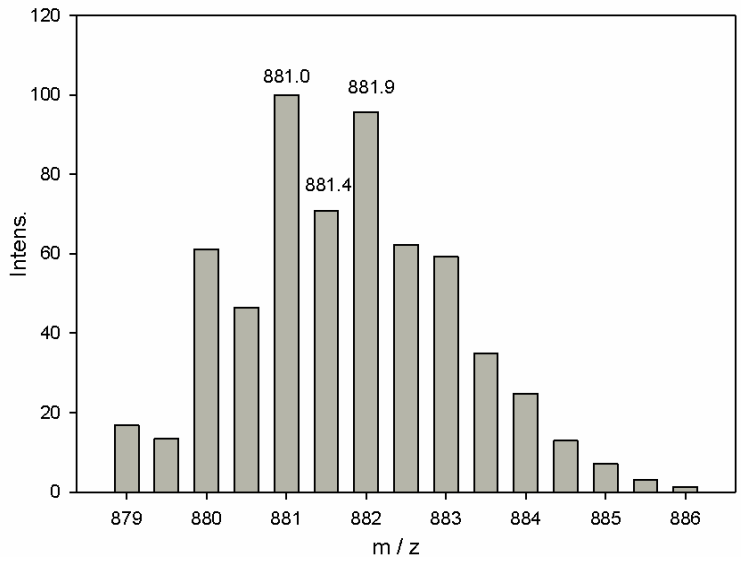

Figure S4 The positive-ion ESI mass spectrum of **1** (upper), and the observed (middle) and calculated (lower) isotopic patterns for $(\mathbf{1} - 2ClO_4^-)^{2+}$ cation.

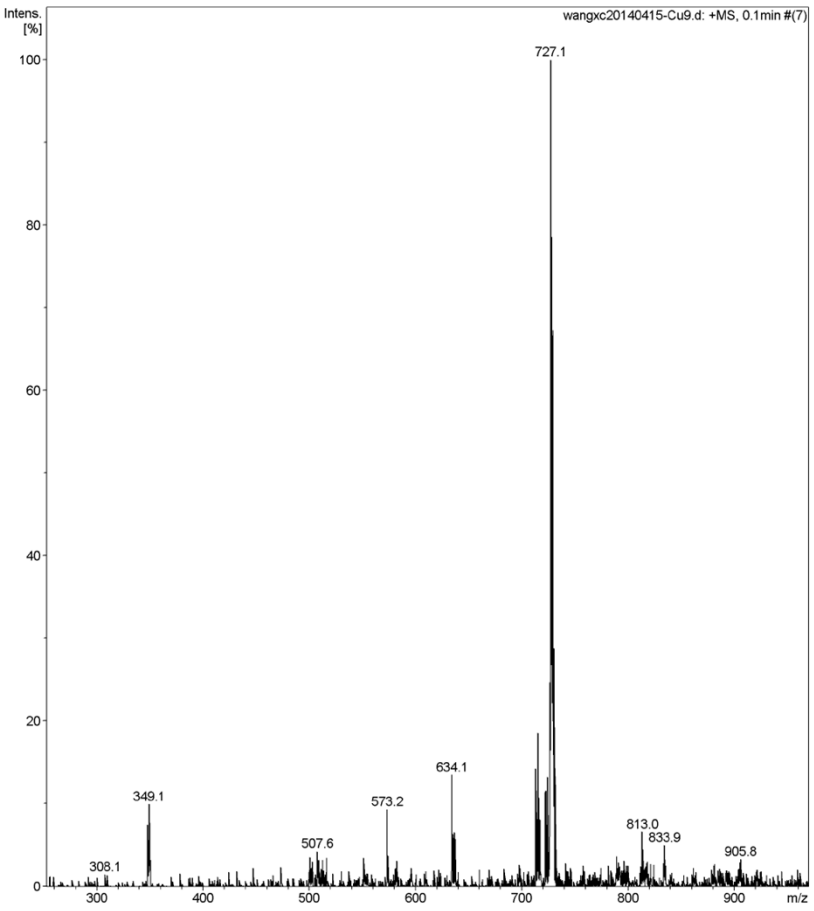

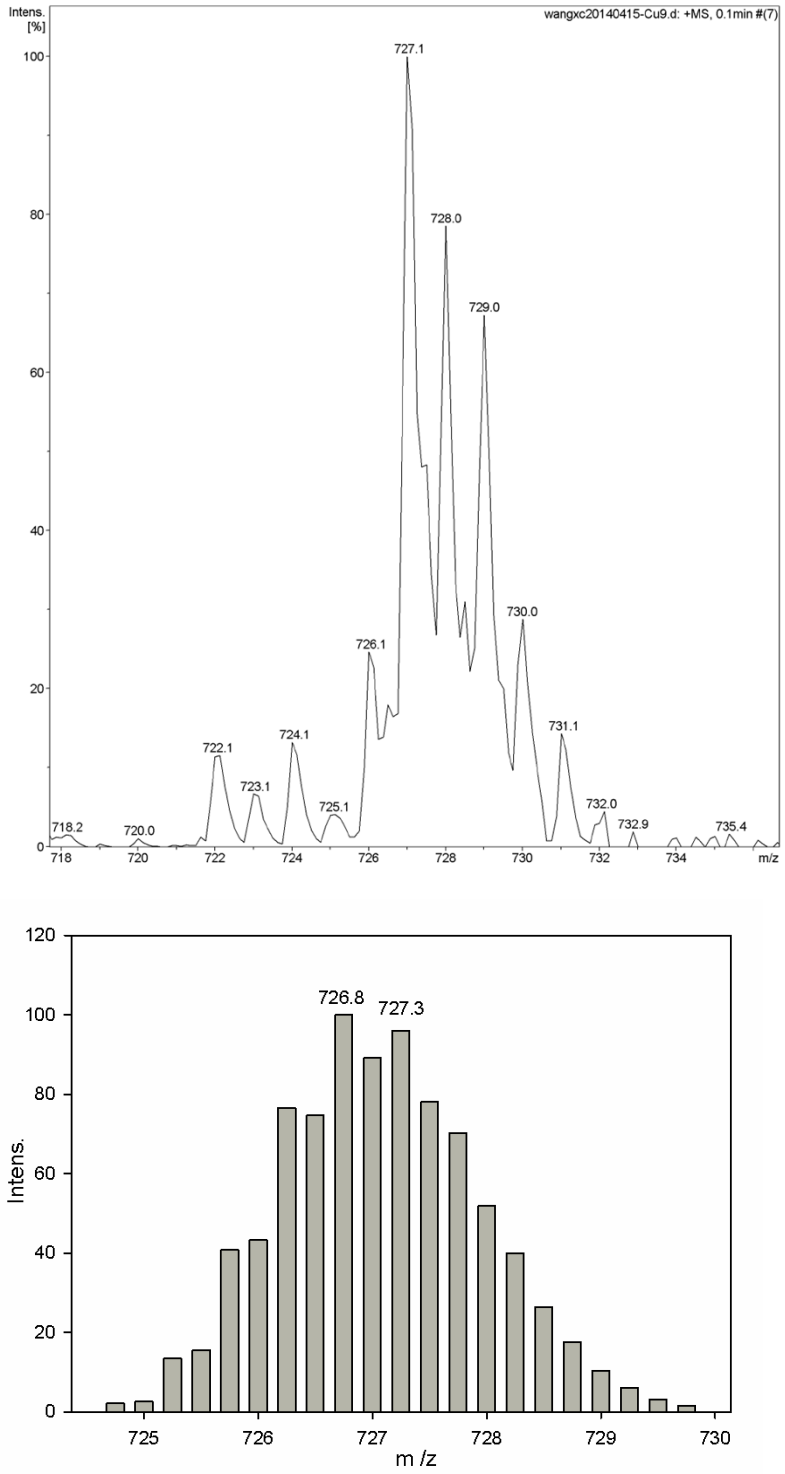

Figure S5 The positive-ion ESI mass spectrum of **2** (upper), and the observed (middle) and calculated (lower) isotopic patterns for $(\mathbf{2} + 4H^{+})^{4+}$ cation.

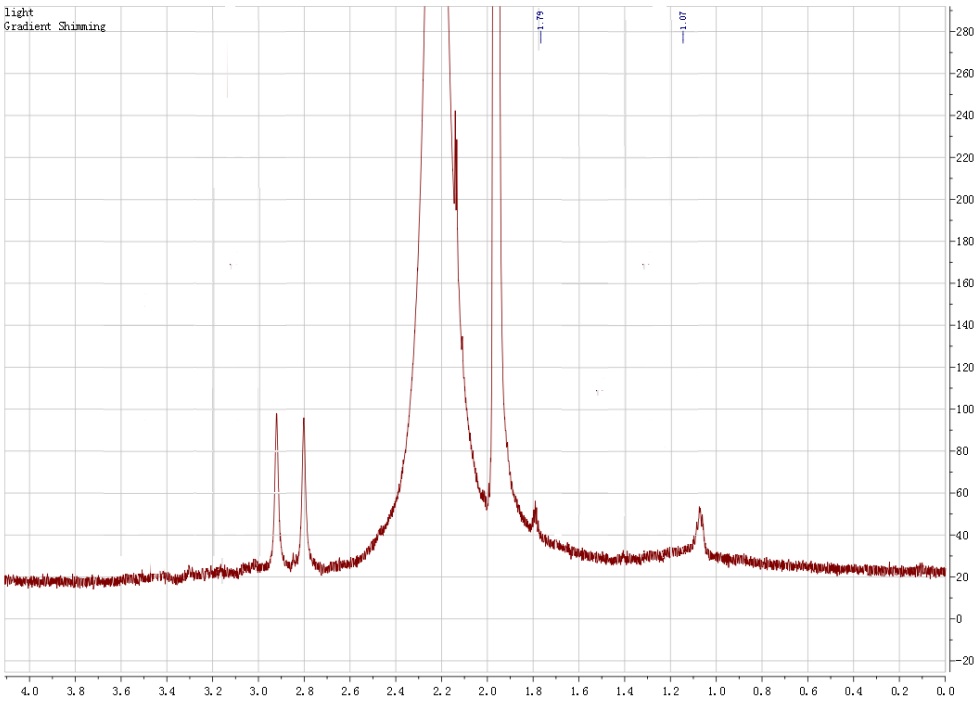

Figure S6 The ^{1}H NMR spectrum of cluster **1** in CD_3CN showing the signals of two types of methyl protons.

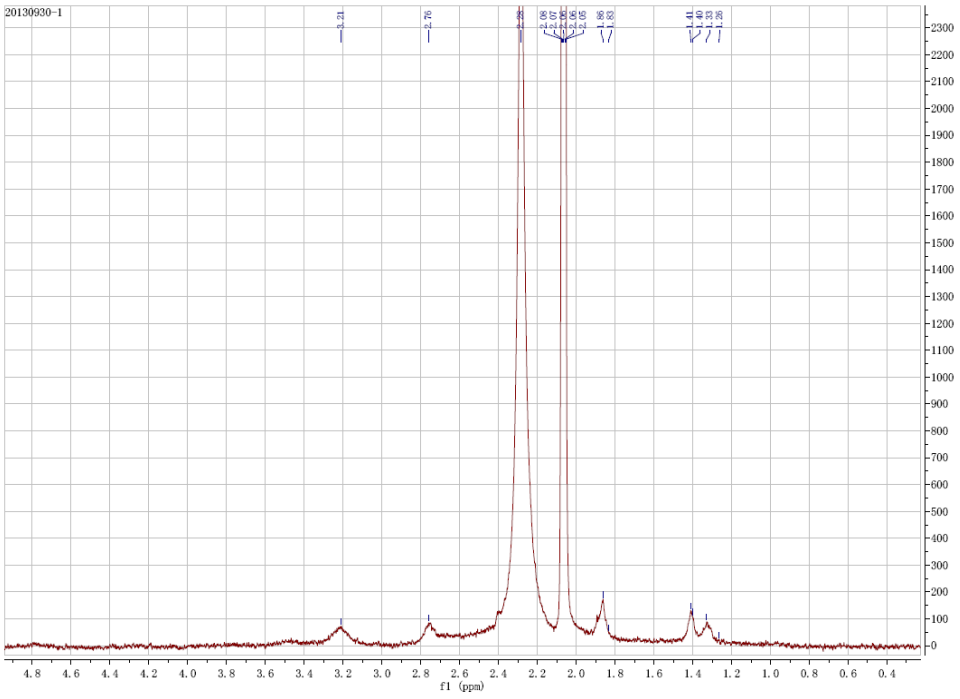

Figure S7 The ^{1}H NMR spectrum of cluster **2** in CD_3CN showing the signals of three types of methyl protons.

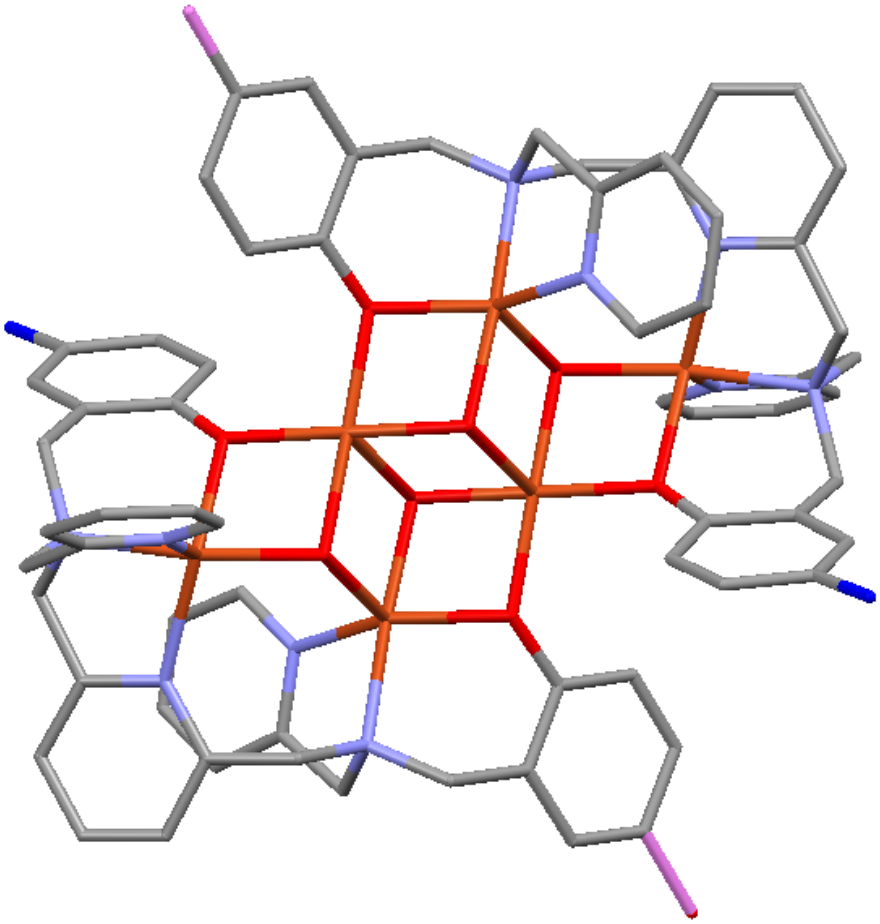

Figure S8 Two types of methyl groups in cluster **1** highlighted in blue and purple, respectively.

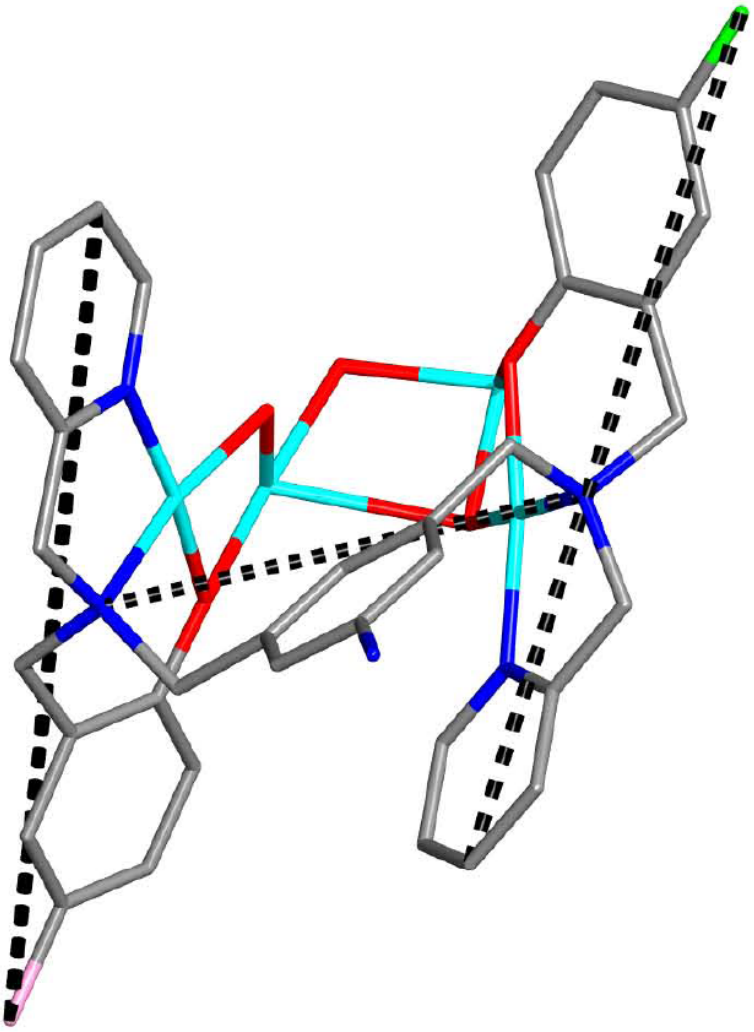

Figure S9 Three types of methyl groups in cluster **2** with methyl groups on the horizontal bar of the twisted "*H*" (blue) and the other two types of methyl groups with similar chemical environment on the vertical bars of the twisted "*H*" (green and purple, respectively). For clarity, only one third of $[Cu_9(\mathbf{L^{II}})_3(OH)_7]$ core was shown.

Alternating current magnetic susceptibility measurements were performed on **1** and **2** in the 2−20 K range under a zero dc field. As shown in Figure S10, no frequency dependence of the ac susceptibility is observed in **1** and **2**. The magnetization versus field curves for **1** and **2** were measured at 2 K under a field of 70 kOe (Figure S11).

As the applied field increases, a rapid increase below about 40 kOe followed by a much slower increase led to a magnetization of 1.86 Nβ for **1** and 2.85 Nβ for cluster **2** at 70 kOe. No inflection point was found in the *M-H* curves at 2 K.

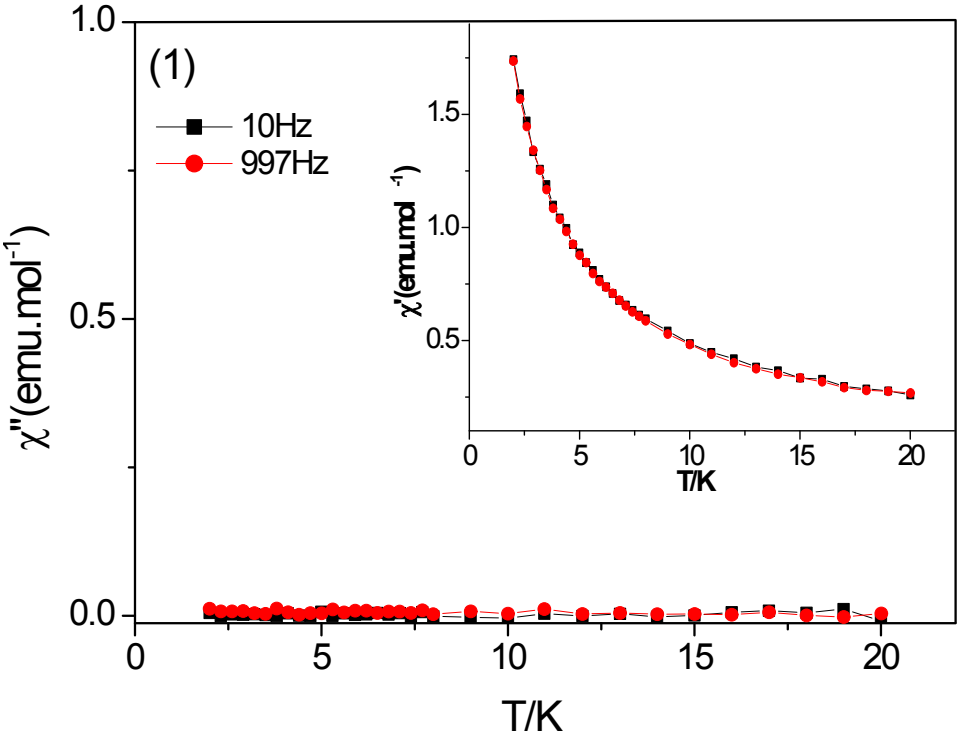

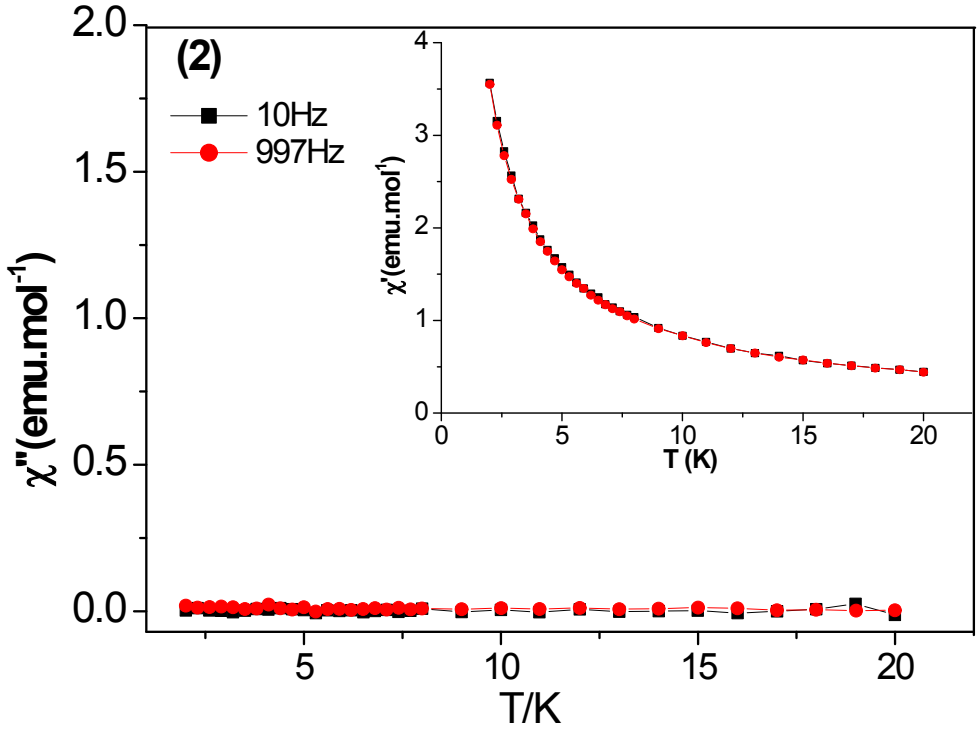

Figure S10 Temperature dependence of the in-phase and Out-of-phase dynamic susceptibility for clusters **1** (above) and **2** (below) under a zero dc field.

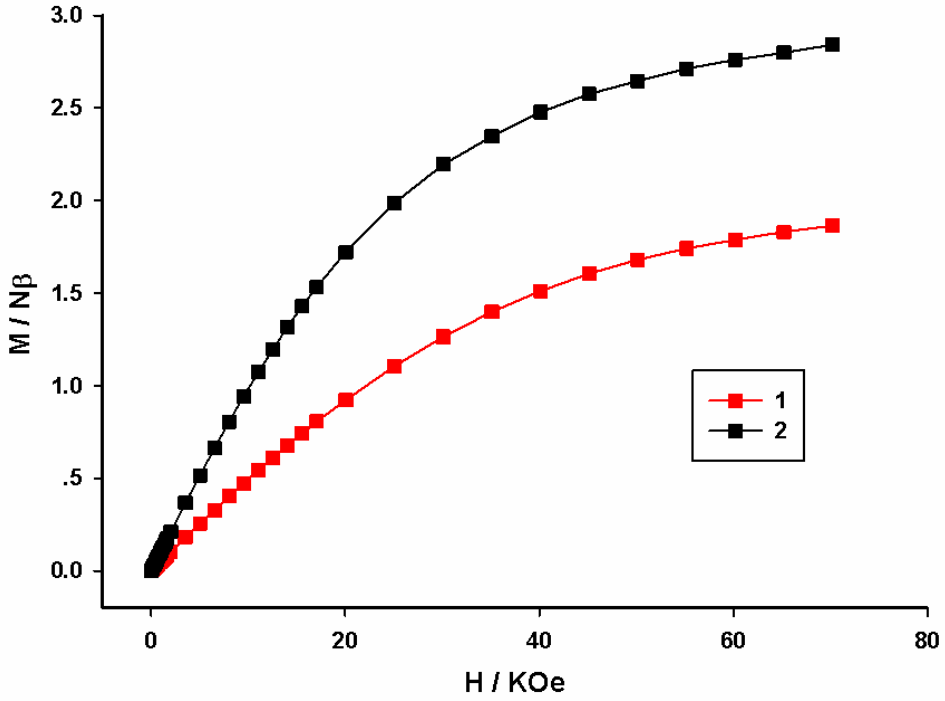

Figure S11 Magnetization data for clusters **1** and **2** at 2 K.

Table S1 Crystallographic data for clusters **1** and **2**.

Complexes	**1**	**2**
Chemical formula	$[C_{70}H_{74}Cu_6N_{10}O_8](ClO_4)_4 \cdot 3(C_4H_{10}O) \cdot 2(C_3H_7NO)$	$[C_{111}H_{121}Cu_9N_{12}O_{13}](ClO_4)_5 \cdot 0.25(CH_3OH) \cdot 1.25(H_2O)$
Fw	2331.04	2926.82
Crystal system	Triclinic	Monoclinic
Space group	P-1	P21/c
a (Å)	12.193(8)	18.9914(16)
b (Å)	13.320(9)	21.3495(18)
c (Å)	19.035(17)	33.231(3)
α (°)	107.282(12)	90
β (°)	96.731(11)	103.9630(10)
γ (°)	107.393(8)	90
V (Å^3)	2744(4)	13075.7(19)
Z	1	4
D_{calc} (g·cm^{-3})	1. 411	1.487
F(000)	1204	5978
μ (Mo Kα, mm^{-1})	1.314	1.613
Total no. of reflns.	13118	95469
θ_{max}	25	25
No. of unique reflns.	8942 [$R_{(int)}$ = 0.0503]	22990 [$R_{(int)}$ = 0.0632]
No. of observed refns	5708	14195
No. of variables	702	1683
R_1, wR_2 (obsd data)	0.0591, 0.1549	0.0530, 0.1536
R_1, wR_2 (all data)	0.1030, 0.1818	0.1035, 0.1868
GOF, S	1.034	1.086
Max./min. peak (e. Å^{-3})	0.670, -0.627	0.934, -0.578

Table S2 Conductivity of complexes with different types at 10^{-3} mol/L in MeCN.

Complexes	Electrolyte type	Conductivity (μs/cm)	The expected values[1]
$[Fe(\mathbf{L^I})](ClO_4)$	1:1	130	92-199
$[Ni(H\mathbf{L^I})](BPh_4)$	1:1	90	92-199,
$[Cu(H_2\mathbf{L^I})](Cl)(PF_6)$	2:1	200	220-300
$[Cu_6(\mathbf{L^I})_2(OH)_4](ClO_4)_4$ (**1**)	4:1	390	500(?)
$[(Cu_9(\mathbf{L^{II}})_3(OH)_7)](ClO_4)_5$ (**2**)	5:1	480	-

[1] GEARY, W. J., *Coordination Chemistry Reviews* **1971**, *7*, 81-122.